Scripta Materialia 69 (2013) 409-412

Experimental Evidence for Non-Cubic Bainitic Ferrite

C. N. Hulme-Smith[a,*], I. Lonardelli[b], A. C. Dippel[c], H. K. D. H. Bhadeshia[a]

[a] *Materials Science and Metallurgy, University of Cambridge, U.K.*
[b] *Materials Engineering and Industrial Technologies, University of Trento, Italy*
[c] *Deutsches Elektronen-Synchrotron DESY, Hamburg, Germany*

Abstract

The first evidence is provided for the existence of a tetragonal or slightly orthorhombic unit cell of bainitic ferrite. It supports the hypothesis that the excess carbon that persists in the ferrite, which is in contact with austenite, is a consequence of an increased solubility due to the change in symmetry from the conventional cubic unit cell. The deviations from the cubic cell are maintained to elevated temperatures, as expected from an increased solubility of carbon in the ferrite.

Keywords: bainite, tetragonal ferrite, orthorhombic ferrite, synchrotron radiation, phase transformations

There has been accumulating and precise evidence that bainitic ferrite that is in prolonged contact with austenite retains a large excess carbon concentration, in spite of the fact that there is an ample opportunity for the carbon to partition into the austenite where it has much greater solubility [1–6]. This phenomenon was attributed originally to the trapping of carbon at imperfections such as dislocations [1, 7] but clear evidence has now emerged that a large fraction of the carbon is in fact in solid solution within the ferrite [8, 9].

It has been proposed that the apparent reluctance of the excess carbon to partition from ferrite which is supersaturated according to the conventional phase diagram, is due to a change in the symmetry of the ferrite unit cell originating from the mechanism of transformation [10]. The transformation to bainite is displacive with the change in lattice from cubic-F to cubic-I achieved by a Bain deformation [11, 12]. The carbon atoms in both the parent and product phases occupy octahedral interstices, but there are three

*Corresponding Author

times as many of these interstices per atom of iron in the ferrite than in austenite. This means that the Bain strain places all the carbon atoms on to one sub-lattice of octahedral interstices in the ferrite when the latter forms without diffusion, resulting in a tetragonal unit cell. The location of carbon atoms on just one set of octahedral interstices is sometimes referred to as Zener order [13], and in this context is a natural consequence of the Bain strain. This leads to a dramatic increase in the solubility of carbon in ferrite that is in equilibrium with austenite [10].

In this work, we present the first experimental evidence indicating that the unit cell of bainitic ferrite is either tetragonal or somewhat orthorhombic, and at the same time, explore its stability to thermal treatment using *in situ* synchrotron X-ray diffraction. Additional evidence for the non-cubic nature of the ferrite crystal structure is provided from laboratory-based X-ray diffraction.

The steel studied *in-situ* is one which exhibits a nanocrystalline bainitic structure as described elsewhere [14, 15] with the chemical composition as stated in Table 1 and is referred to as alloy 1. The structure consists of fine platelets of bainitic ferrite in a matrix of residual austenite, produced by austenitisation at 930 °C for 30 min followed by isothermal transformation at 200 °C for 10 days. The austenite is enriched in carbon relative to the average composition of the steel, due to the partial partitioning of carbon from the bainite when it first forms by a diffusionless mechanism. Numerous metallographic studies are available elsewhere and are not reproduced here for the sake of brevity [15, 16].

Table 1: Composition (wt%) of alloy 1 studied during *in situ* heating.

C	Mn	Si	Co	Cr	Mo	V	Cu
0.84	2.26	1.78	1.55	1.47	0.25	0.11	0.106
Nb	Sn	S	Al	Ni	Ti	B	N
0.021	0.019	0.008	0.043	0.036	0.011	0.0003	0.003

A sample of alloy 1, heat-treated to produce nanostructured bainite, was examined using synchrotron X-ray diffraction on the Petra III P02.1 beamline at DESY, Germany. The wavelength of the radiation was 0.2069 Å, monochromated using diamond and silicon {111} planes. Instrument parameters were fixed using a ceria standard. The parameters

were checked using the spectrum from a Si standard and the fit was found to be satisfactory. The sample was heated as per Figure 1a, using a hot air gun. The temperature was measured using a thermocouple, with manual adjustment of the gas jet to achieve the desired conditions.

Each spectrum was recorded over 30 s throughout the 3 h heat treatment using a flat 2D solid-state detector mounted perpendicular to the incident beam. The data were analysed using the Materials Analysis Using Diffraction (MAUD) program [17, 22, 23]. Data were recorded as 2D TIFF images with 32 bit dynamic range and were integrated over 360°using ImageJ plugins within MAUD. It was observed that the peaks in spectra converted from the ceria and silicon standards, which both have face-centred cubic crystal structures, were symmetrical and well-fitted using a face-centred cubic phase during Rietveld refinement. An example spectrum is presented in Figure 1b. Each spectrum was fitted using a Rietveld refinement assuming that there were only two expected phases present: austenite and ferrite. Three independent sets of analysis were performed, one imposing a body-centred cubic lattice ($\mathrm{Im}\bar{3}\mathrm{m}$) for ferrite, another imposing body-centred tetragonal ferrite lattice ($\mathrm{I}\frac{4}{m}\mathrm{mm}$) and one imposing a body-centred orthorhombic lattice (I222) on ferrite. For completeness, both face-centred cubic and face-centred orthorhombic crystal structures were trialled for austenite, the latter producing no significant change in fit from the former. It was concluded that the austenite was face-centred cubic (Figure 2).

The polynomial background function, total incident X-ray intensity, austenite phase fraction (the residue being ferrite), microstrain, crystallite size and applicable lattice parameters were allowed to refine. The weighted profile factor, R_{wp}, is considered to be the most relevant to follow the progress of structure refinement [18], where

$$R_{\mathrm{wp}} = \left[\frac{\Sigma w_i (x_i - y_i)^2}{\Sigma w_i x_i^2}\right]^{1/2} \tag{1}$$

where x_i is the discrete observed intensity and y_i the corresponding calculated intensity. w_i is the observation weight, assigned the value x_i^{-1}. The values of R_{wp} for each ferrite crystal structure are plotted throughout the heat treatment in Figure 4a. It is evident that the fit to the experimental data is much better assuming a non-cubic ferrite unit cell (Figure 2), and that the R_{wp} values for all three symmetries converge as the experiment

progresses (Figure 4). This is expected, since the cubic symmetry is gradually restored due to the slow partitioning of carbon throughout the heat treatment. The evolution of the tetragonal ferrite unit cell parameters, a_t and c_t and the ratio c_t/a_t, are given in Figure 3a, along with the plot of evolution of the orthorhombic lattice parameters, a_o, b_o and c_o in Figure 3b. It is noted that the austenite lattice parameter and volume fraction are negligibly sensitive to the symmetry of the ferrite unit cell (Figure 4b). The lattice parameters of austenite and ferrite show significant contractions beyond 2 h, corresponding to a temperature of $\approx 600\,^{\circ}\mathrm{C}$ when the austenite begins to decompose into carbides and ferrite, leading to a contraction in lattice parameter [19].

The lattice parameter ratio of martensite in steel, c_t/a_t, depends on the carbon concentration according to the relationship $c_t/a_t = 1+0.045x_w$ where x_w is the concentration of carbon in wt% [20, 21]. Using the initial value of $c_t/a_t = 1.0086$ for tetragonal ferrite (Figure 3a), this yields a *dissolved* carbon concentration of 0.19 wt%, which is in good agreement with the atom probe data reported by Caballero and coworkers [8, 9]. Even more interesting is that the tetragonality persists to considerable temperatures, indicating once again the reluctance of the carbon to leave the ferrite and partition into the austenite, consistent with the work indicating that the solubility of carbon in tetragonal ferrite that is in contact with austenite is much greater than is the case for cubic ferrite.

As stated earlier, the Bain strain renders a random distribution of carbon atoms into austenite into one that is ordered on a single sub-lattice of octahedral interstices in the ferrite when the transformation occurs without diffusion, leading to the classical tetragonality. However, it is possible to obtain orthorhombic symmetry, as has been reported in some martensites (reviewed in [21]), because a fraction of the carbon atoms are shuffled by the lattice invariant deformation, whether that is slip or twinning. Therefore, the possibility of an orthorhombic cell was also investigated; even though a predicted phase diagram is not available for this case, there is no reason to suppose that it would not lead to enhanced solubility similar to the tetragonal case. The fit parameter R_{wp} is improved slightly by assuming an orthorhombic cell (Figure 4a), and the initial asymmetries prior to heating of $c_o/a_o = 1.012$ and $b_o/a_o = 1.007$. The implications of these particular values are not yet clear.

Both alloy 1 and another alloy, alloy 2, with the composition detailed in Table 2

investigated using laboratory-based X-ray diffraction (alloy 2 was austenitised at 1050°C for 30 min, followed by isothermal transformation at 250°C for 3 days). A scan was performed using a Philips PW1820 diffractometer with a graphite monochromator and Bragg Brentano parafocusing geometry. During the experiment, $40^\circ < 2\theta < 125^\circ$ with a step size of 0.02°. The dwell time was 10 s. Additional information is given in Supplementary Table 1 and the spectra obtained is given in Supplementary Figure 1 and 2. The results for alloy 1 are given in Supplementary Table 2 and those for alloy 2 are detailed in Supplementary Table 3. Parameters were derived for this diffractometer from a silicon standard and were used for all subsequent Rietveld analysis.

The results obtained in the synchrotron were corroborated with similar reductions in R_{wp}. Using a body-centred tetragonal crystal structure for ferrite in Rietveld analysis resulted in a $c_{\mathrm{t}}/a_{\mathrm{t}}$ ratio of 1.0073 ± 0.0002 and a body-centred orthorhombic structure gives a $c_{\mathrm{o}}/a_{\mathrm{o}}$ ratio of 1.0101 ± 0.0004 and $b_{\mathrm{o}}/a_{\mathrm{o}}$ of 1.0085 ± 0.0004.

Alloy 2 exhibits the same type of microstructure as the alloy 1 and was examined using a scan ranging from $2\theta = 40^\circ$ to $2\theta = 125^\circ$. A tetragonal ferrite crystal structure leads to a c/a ratio of 1.0062 ± 0.0003, and provides a better fit than cubic symmetry to the data. This, in turn, leads to a calculated carbon content in the ferrite of 0.16 wt% [20, 21]. The carbon content of the ferrite in the sample of alloy 2 may be expected to be lower since the isothermal transformation temperature was higher, which would allow more partitioning of carbon away from the ferrite. Using an orthorhombic crystal structure for ferrite further reduces the R_{wp} value and results in a $c_{\mathrm{o}}/a_{\mathrm{o}}$ ratio of 1.0093 ± 0.0011 and a $b_{\mathrm{o}}/a_{\mathrm{o}}$ ratio of 1.0085 ± 0.0011. The refined values of b_{o} and c_{o} lie within error of each other.

Table 2: Composition (wt%) of alloy 2.

C	Mn	Si	Al	Mo
1.037	1.97	3.89	1.43	0.24

It has been demonstrated that the carbon that persists in solid solution within the bainitic ferrite following prolonged isothermal transformation at 200 °C is sufficiently Zener-ordered [13] to cause the ferrite unit cell to be non-cubic. The present analysis is

probably more consistent with the orthorhombic form although the difference with the tetragonal cell on the basis of fit to experimental data may not be significant. However, the results obtained here suggest that an appropriate phase diagram must be used when commenting on the equilibrium solubility of carbon in ferrite. It is hoped to take these concepts further with more *in situ* experiments designed for greater confidence.

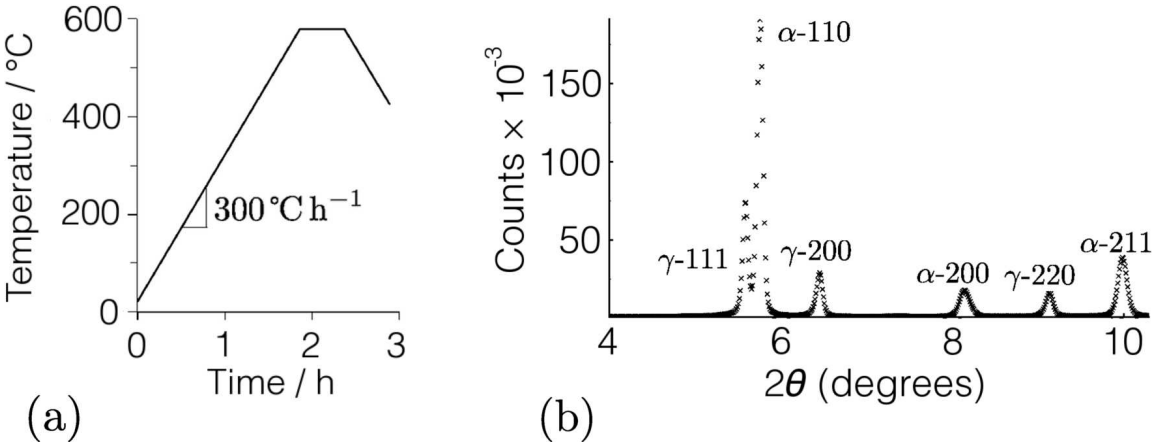

Figure 1: a) Heat treatment implemented in the synchrotron. After 3 hours, the sample was allowed to air cool. b) Indexed X-ray diffraction spectrum recorded during the experiment.

Scripta Materialia 69 (2013) 409-412

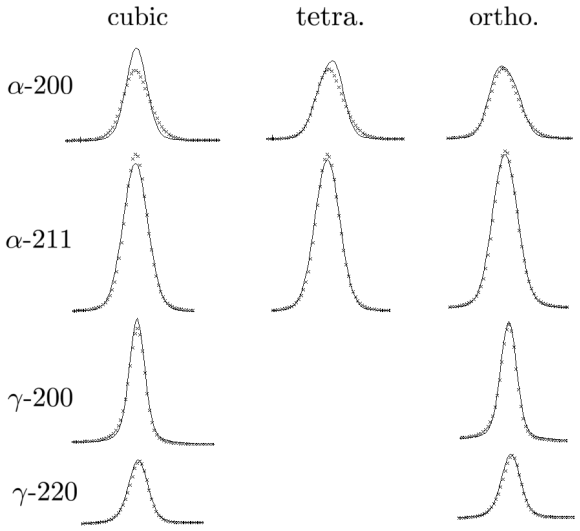

Figure 2: Examples of peaks from synchrotron X-ray spectra, fitted using the crystal structures indicated.

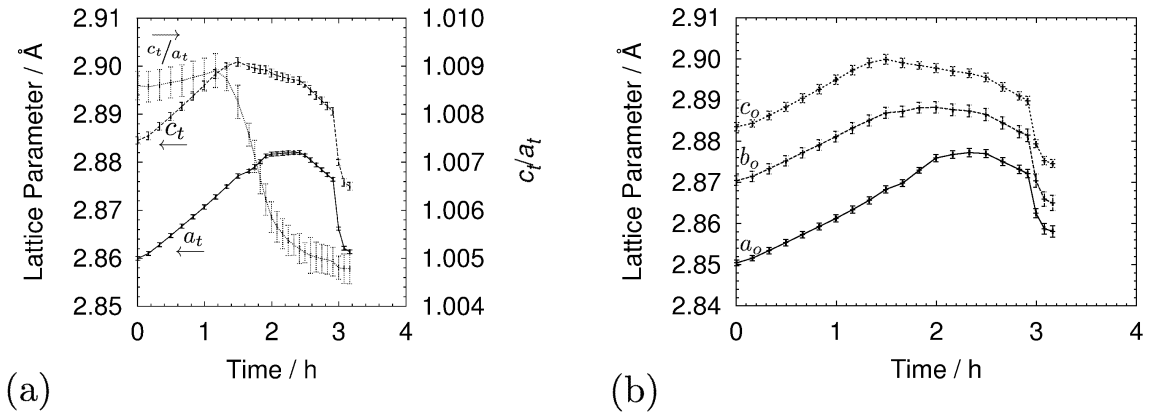

Figure 3: Lattice parameters of a) tetragonal ferrite, b) othorhombic ferrite.

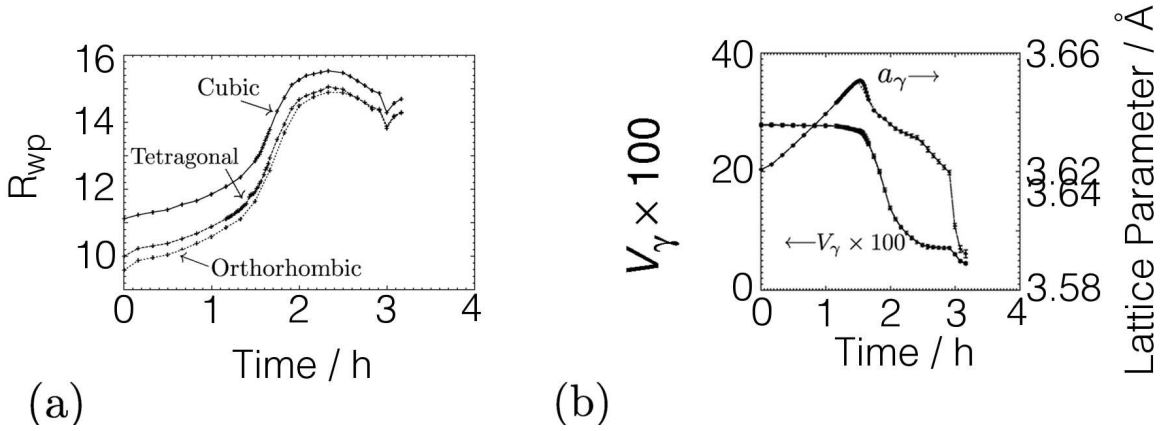

Figure 4: a) Parameter which is small when the Rietveld fit to the full profile is better. Plotted as a function of time during heat treatment in the synchrotron experiment. b) Austenite lattice parameter and volume fraction. The results for all ferrite crystal structures are plotted.

References

[1] H. K. D. H. Bhadeshia, A. R. Waugh: Acta Metall. 30 (1982) 775.

[2] M. Peet, S. S. Babu, M. K. Miller, H. K. D. H. Bhadeshia: Scr. Mater. 50 (2004) 1277.

[3] F. G. Caballero, M. K. Miller, S. S. Babu, C. Garcia-Mateo: Acta Mater. 55 (2007) 381.

[4] C. Garcia-Mateo, M. Peet, F. G. Caballero, H. K. D. H. Bhadeshia: Mat. Sci. Techn. 20 (2004) 814.

[5] F. G. Caballero, M. K. Miller, A. J. Clarke, C. Garcia-Mateo: Scr. Mater. 63 (2010) 442.

[6] I. B. Timokhina, X. Y. Xiong, H. Beladi, S. Mukherjee, P. D. Hodgson: Mat. Sci. Techn. 27 (2011) 739.

[7] H. K. D. H. Bhadeshia, A. R. Waugh: An atom–probe strudy of bainite: in: H. I. Aaronson, D. E. Laughlin, R. F. Sekerka, C. M. Wayman (Eds.), Solid-Solid Phase Transformations: TMS–AIME, Warrendale, Pennsylvania, USA, 1982: pp. 993.

[8] F. G. Caballero, M. K. Miller, C. Garcia-Mateo, J. Cornide: Journal of Alloys and Compounds (2012) doi:10.1016/j.jallcom.2012.02.130.

[9] F. G. Caballero, M. K. Miller, C. Garcia-Mateo, J. Cornide, M. J. Santofimia: Scr. Mater. 67 (2012) 846.

[10] J. H. Jang, H. K. D. H. Bhadeshia, D. W. Suh: Scr. Mater. 68 (2012) 195.

[11] E. C. Bain: Trans. AIME 70 (1924) 25.

[12] H. K. D. H. Bhadeshia: Bainite in Steels, 2nd edition: Institute of Mat., London, U.K., 2001.

[13] J. C. Fisher, J. H. Hollomon, D. Turnbull: Met. Trans. 185 (1949) 691.

[14] F. G. Caballero, H. K. D. H. Bhadeshia, K. J. A. Mawella, D. G. Jones, P. Brown: Mat. Sci. Techn. 18 (2002) 279.

[15] H. K. D. H. Bhadeshia: Proc. Roy. Soc. A 466 (2010) 3.

[16] H. K. D. H. Bhadeshia: Archive of micrographs, (2005).
URL `http://www.msm.cam.ac.uk/phase-trans/2005/bulk.html`

[17] L. Lutterotti: Mat. analysis using diffraction (2013).
URL `http://www.ing.unitn.it/ maud/index.html`

[18] J. I. Langford, D. Louër: Rep. on Prog. Phys. 59 (1996) 131.

[19] J. Y. Chae, J. H. Jang, G. Zhang, K. H. Kim, J. S. Lee, H. K. D. H. Bhadeshia, D. W. Suh: Scr. Mater. 65 (2011) 245.

[20] E. Honda, Z. Nishiyama: Sci. Rep. of Tohoku Imp. Uni. 21 (1932) 299-.

[21] J. W. Christian: Mat. Trans., JIM 33 (1992) 208.

[22] L. Lutterotti, S. Matthies,H. R. Wenk, A. S. Schultz, J. W. Richardson: J. App. Phys. 21 (1997) 594

[23] L. S. Lutterotti, S. Matthies, H. R. Wenk: IUCr-CPD Newsl. 21 (1999)